Engineering Fracture Mechanics 214 (2019) 544–557

Contents lists available at ScienceDirect

Engineering Fracture Mechanics

journal homepage: www.elsevier.com/locate/engfracmech

A non-local stress fracture criterion accounting for the anisotropy of the fracture toughness

Marek Romanowicz*

Department of Mechanical Engineering, Bialystok University of Technology, Poland

ARTICLE INFO

Keywords:
Non-local fracture criterion
Mixed-mode fracture
T-stress
Wood
Anisotropy

ABSTRACT

A comparative assessment between the maximum circumferential stress criterion and the non-local stress criterion applied to mixed mode fracture problems in wood is presented. Various attributes of the two fracture theories, such as the shear stress component acting on the critical plane, the non-singular term of the crack tip stress field and the angular distribution of the fracture toughness, are investigated for their impact on the mixed mode fracture behavior of wood. Predictions of the direction of crack propagation and the fracture locus are validated against experimental data available in the literature, with emphasis on results obtained from single edge-notched wood specimens subjected to on-axis biaxial loading and off-axis tensile and off-axis shear loading.

1. Introduction

Cracks in wood structures are most often subjected to mixed mode loading due to either wood anisotropy or external loading conditions. Developing an efficient and reliable mixed mode criterion for wood continues to remain a challenge. Such a criterion should be able to predict both the direction of crack propagation and the critical loads based on the physics laws. Moreover it should be validated against experimental results for different crack inclinations with respect to the orthotropy axes and for different loading mode mixities.

The classical way of analyzing crack problems in wood and other orthotropic materials is based on the two main assumptions that a crack is treated as a zero thickness discontinuity with stress singularities at the crack tips and that the rest of material is a continuum. Van der Put [1] has proposed for wood a new fracture theory that abandons these assumptions and considers an small elliptic crack in the isotropic matrix. The author developed a mixed mode fracture criterion in terms of matrix stresses at the boundary of the crack and proposed a orthotropic-isotropic transformation to apply it for wood. The concept of orthotropic-isotropic transformation has been adopted by Fakoor's group [2–4] as the starting point to develop a new formulation for the strain energy release rate criterion based on the fracture properties of the isotropic matrix. Because the applicability of van der Put's theory for long cracks crossing the reinforcement is considered to be controversial, the classical approach is still commonly used.

The main focus of the classical approach is to extend the isotropic fracture criteria into orthotropic materials. Fracture criteria in the form used for isotropic materials are inadequate to predict the crack propagation direction for orthotropic materials. For example, the maximum circumferential stress theory proposed by Erdogan and Sih [5] as well as the non-local stress theory formulated by Seweryn and Mroz [6] predict that a crack located along the reinforcement direction under pure mode I loading propagates in the direction approximately 50° away from the original crack plane, which is inconsistent with experimental observations. This

* Address: Wiejska 45C, 15–351 Bialystok, Poland.
E-mail address: m.romanowicz@pb.edu.pl.

https://doi.org/10.1016/j.engfracmech.2019.04.033
Received 8 January 2019; Received in revised form 12 March 2019; Accepted 26 April 2019
Available online 01 May 2019

inconsistency can be fixed, in two different ways, by taking the anisotropy of the fracture toughness into account or by abandoning the maximization of some failure functions. The first method, developed by Buczek and Herakovich [7] and Saouma et al. [8], has become a standard technique for fracture analyses of fiber reinforced composites [9–14]. The latter method, motivated by observations of cracking in fiber reinforced composites, is based on a concept of weak planes parallel to the reinforcement direction [15–18]. The use of the latter method, in practice, means that the crack propagation angle is found empirically. Parallel to the theoretical studies, a number of empirical studies have attempted to establish formulae for mixed mode crack problems in wood [19–21].

The objective of this paper is to show that it is possible to predict both the direction of crack propagation and the critical loads in wood by using the non-local stress fracture criterion accounting for the anisotropy of the fracture toughness. In particular, the utility of the new approach for solving crack problems in wood and its advantages and disadvantages in comparison with the maximum circumferential stress theory are discussed. To date, only the simplified version of the non-local stress fracture criterion, which does not require the maximization, has been presented by Romanowicz and Seweryn [16].

2. Orthotropic fracture criteria

Consider a two-dimensional linear elastic fracture problem of orthotropic body with a crack. The most general case of crack configuration, when a crack axis does not coincide with an axis of orthotropy, is shown in Fig. 1. The stress components in a polar coordinate system originated at the crack tip are related to the stress components in a rectangular coordinate system as follows

$$\sigma_\theta = \sigma_x \sin^2\theta + \sigma_y \cos^2\theta - 2\tau_{xy}\sin\theta\cos\theta \tag{1}$$

$$\tau_{r\theta} = -\sigma_x \sin\theta\cos\theta + \sigma_y \sin\theta\cos\theta + \tau_{xy}(\cos^2\theta - \sin^2\theta) \tag{2}$$

The asymptotic stress fields in the vicinity of the crack tip in a orthotropic material are given in Appendix. The stress singularity close to the crack tip is described by the opening and sliding mode stress intensity factors, i.e. K_I, K_{II}.

The maximum circumferential stress fracture criterion, formulated by Erdogan and Sih [5], states that crack propagation takes place when the circumferential tensile stress at some distance from the crack tip r_c reaches the critical value σ_c

$$\max\left(\frac{\sigma_\theta}{\sigma_c}\right) = 1 \tag{3}$$

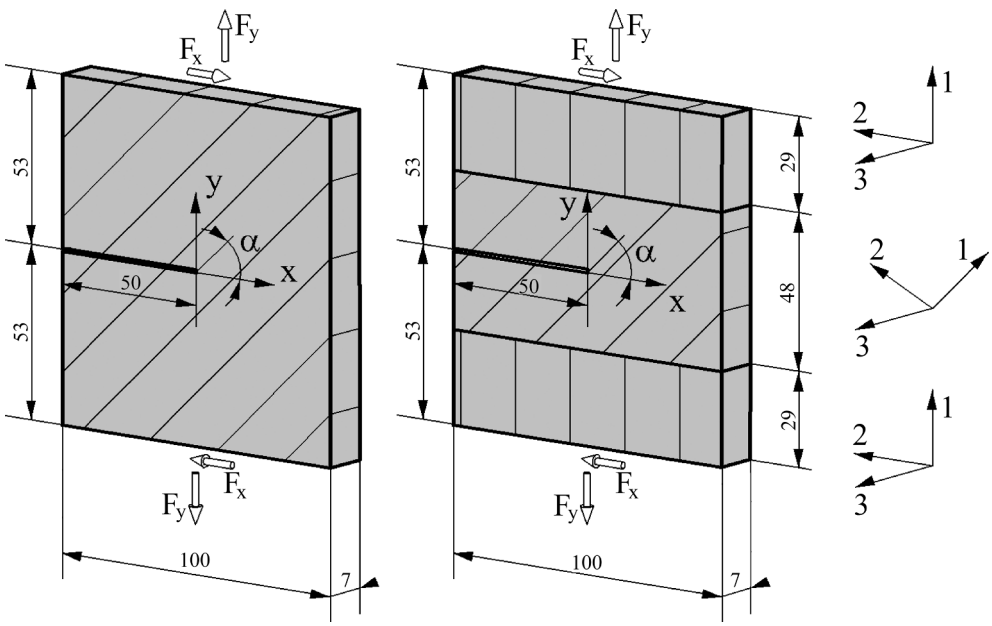

Fig. 1. Specimen geometries used in the analysis (dimensions in mm).

This theory assumes that a crack propagates in the direction θ_c where the circumferential tensile stress is maximum. The authors suggested that the critical value σ_c can be determined by using the Griffith-Irwin fracture criterion, $K_I = K_{Ic}$ for the opening crack mode. Substituting circumferential stress (1) into (3) and assuming $\theta_c = 0^\circ$, the Griffith-Irwin condition is equivalent to

$$\sigma_c = \frac{K_{Ic}}{\sqrt{2\pi r_c}} \tag{4}$$

where K_{Ic} is the mode I fracture toughness. Using the Eqs. (1), (3) and (4), the fracture criterion of a orthotropic material can be written for mixed fracture mode problems in the linear form

$$b_0\sqrt{2\pi r_c}\,T + b_1 K_I + b_2 K_{II} = K_{Ic} \tag{5}$$

where T denotes the non-singular term of the crack tip stress field and coefficients b_0, b_1 and b_2 depend on material properties and crack inclination with respect to the orthotropy axes.

Note that the maximum circumferential stress fracture theory neglects the effect of shear stress on material decohesion. To assess this effect, the non-local stress fracture theory proposed by Seweryn and Mroz [6] is used in this work. This approach states that crack propagation occurs when the function $R(\sigma_\theta, \tau_{r\theta})$ of normal and shear stresses acting on a physical plane averaged over a length of damage zone d reaches the maximum value

$$\max\left[\frac{1}{d}\int_0^d R(\sigma_\theta, \tau_{r\theta})dr\right] = 1 \tag{6}$$

Thus, the crack propagation angle θ_c is found by maximization of the function $R(\sigma_\theta, \tau_{r\theta})$. The authors suggested that the length d can be determined by using the Griffith-Irwin fracture criterion, $K_I = K_{Ic}$ for the opening crack mode. Substituting circumferential stress (1) into (6) and assuming $\theta_c = 0^\circ$, it is possible to compute the length of damage zone

$$d = \frac{2}{\pi}\left(\frac{K_{Ic}}{\sigma_c}\right)^2 \tag{7}$$

For a material with growing microcracks, Seweryn et al. [22,23] proposed the following damage model

$$R(\sigma_\theta, \tau_{r\theta}) = \sqrt{\left(\frac{\sigma_\theta}{\sigma_c}\right)^2 + c\left(\frac{\tau_{r\theta}}{\sigma_c}\right)^2} \tag{8}$$

where σ_c is the tensile strength, c represents the ratio of the extensional and sliding compliance of a body weakened by microcracks. Lacking experimental data for c, it can be taken equal to the ratio of the critical values of stress intensity factors for the opening and sliding fracture modes

$$c = \left(\frac{K_{Ic}}{K_{IIc}}\right)^2 \tag{9}$$

However, the use of T-stress in the elliptical condition (8) makes it cumbersome to manipulate. Thus, only singular stress terms are considered in the non-local stress fracture theory. Using the equations (1), (2) and (6)–(9), the non-local stress fracture criterion for a orthotropic material can be expressed in terms of stress intensity factors as

$$\lambda_{11}(K_I)^2 + \lambda_{12}K_I K_{II} + \lambda_{22}(K_{II})^2 = (K_{Ic})^2 \tag{10}$$

where coefficients λ_{11}, λ_{12} and λ_{22} depend on material properties and crack inclination with respect to the orthotropy axes. They satisfy the inequality $(\lambda_{12})^2 - 4\lambda_{11}\lambda_{22} < 0$. Thus, neglecting the T-stress, the relation obtained from the non-local stress fracture criterion for mixed fracture mode problems is a rotated ellipse that is located in the center of the K_I, K_{II} system. It should be noted that the elliptical criterion (10) predicts two possible solutions in the system of stress intensity factors.

For orthotropic materials, fracture criteria in the form (5) and (10) fail to predict the crack propagation angle θ_c accurately. In order to overcome this limitation, two approaches are used in this work. The first method, proposed by Jernkvist [15] and Romanowicz and Seweryn [16], postulates a concept of weak planes parallel to the reinforcement direction. Thus, the crack propagation angle in orthotropic materials is given a priori by the reinforcement direction.

$$\theta_c = \alpha \text{ or } \alpha - 180^\circ \tag{11}$$

and there is no need to compute the maxima of functions (3) and (6). In this approach, K_{Ic} means the mode I fracture toughness for a crack located along the reinforcement direction. The second method, proposed by Buczek and Herakovich [7] and Saouma et al. [8] introduces a modification to criteria (3) and (6) by replacing a fixed K_{Ic} with a value $K_{Ic}^{(\theta)}$ which represents the fracture toughness on the θ plane.

$$K_{Ic}^{(\theta)} = K_{Ic}^{(2)}\cos^2\theta + K_{Ic}^{(1)}\sin^2\theta \tag{12}$$

where $K_{Ic}^{(1)}$ and $K_{Ic}^{(2)}$ are the mode I fracture toughness along the 1 and 2 orthotropy axes, respectively. Note that $K_{Ic}^{(1)}$ refers to a crack oriented across the reinforcement direction wheras $K_{Ic}^{(2)}$ corresponds to a crack oriented along the reinforcement direction. In the case of cracks inclined to the 1 axis by an angle α, the angular variation of the fracture toughness is given by

$$K_{Ic}^{(\theta)} = K_{Ic}^{(2)}\cos^2(\theta-\alpha) + K_{Ic}^{(1)}\sin^2(\theta-\alpha) \tag{13}$$

Lacking experimental data for $K_{Ic}^{(1)}$, the authors suggested that the ratio of the fracture toughness along the 1 and 2 orthotropy axes can be considered equal to the ratio of the corresponding elastic moduli

$$\frac{K_{Ic}^{(1)}}{K_{Ic}^{(2)}} = \frac{E_1}{E_2} \tag{14}$$

Substituting (14) into (13), $K_{Ic}^{(\theta)}$ can be expressed as

$$K_{Ic}^{(\theta)} = K_{Ic}^{(2)}\left[\cos^2(\theta-\alpha) + \frac{E_1}{E_2}\sin^2(\theta-\alpha)\right] \tag{15}$$

or if the missing value is $K_{Ic}^{(2)}$

$$K_{Ic}^{(\theta)} = K_{Ic}^{(1)}\left[\frac{E_2}{E_1}\cos^2(\theta-\alpha) + \sin^2(\theta-\alpha)\right] \tag{16}$$

It should be noted that Eqs. (15) and (16) produce the same locations of the maxima of functions (3) and (6).

3. Evaluation of the stress intensity factors and T-stress

In order to verify the accuracy of the orthotropic fracture theories, theoretical predictions are compared with experimental results of mixed mode fracture of pine wood (Pinus silvestis) in the LR orthotropy plane reported by Romanowicz and Seweryn [16]. The authors performed three types of fracture tests on single edge-notched specimens. For the first test problem, the reinforcement direction coincided with the crack axis and the specimens were subjected to various combinations of tensile and shear loading. The loading combinations were defined by seven loading angles $\chi = 0^\circ, 15^\circ, 30^\circ, 45^\circ, 60^\circ, 75^\circ$ and 90°. The shear and tensile components of the load F are calculated as follows

$$F_x = F\sin\chi, \quad F_y = F\cos\chi \tag{17}$$

For the next two test problems, the reinforcement direction was rotated by an angle α with respect to the crack axis and the specimens were subjected to tensile and shear loading, separately. The material orientation were defined by five rotation angles $\alpha = 0^\circ, 22.5^\circ, 45^\circ, 67.5^\circ$ and 90°. They used two types of single edge-notched specimens, namely, consisted of one piece of wood if tensile loading was applied and glued from three pieces of wood if shear loading occurred. Material properties of wood and specimen geometries used in the fracture analysis are shown in Table 1 and Fig. 1. Two-dimensional finite element models of the specimens under a plane stress condition were generated. The crack tip region was meshed with the singular quarter point elements with length equal to $a/77$. Using ANSYS finite element code and displacement extrapolation method, stress intensity factors and T-stress were evaluated. Details of the method are given in Appendix. Figs. 2 and 3 show the results of computations for different α. Variations of the stress intensity factors and T-stress are normalized by the tensile F_y and shear F_x forces acting at the top and bottom of the specimen. It is interesting to note that the stress intensity factors are positive and T-stress negative for crack inclinations used in the experiments. The fracture toughness and real value of T-stress can be estimated by scaling the normalized values linearly with the failure load of specimen presented in Ref. [16]. In order to describe the contribution of non-singular stress, the T-stress values are converted to a non-dimensional form by using the relation proposed by Leevers and Radon [24]

$$B = \frac{T\sqrt{\pi a}}{\sqrt{K_I^2 + K_{II}^2}} \tag{18}$$

The values of the biaxial parameter B for different material orientations α and two loading modes are shown in Table 2.

Table 1
Material parameters used in the analysis.

E_1 (GPa)	E_2 (GPa)	G_{12} (GPa)	ν_{12}	$\sigma_c^{(2)}$ (MPa)	$K_{Ic}^{(2)}$ (MPam0.5)	$K_{IIc}^{(2)}$ (MPam0.5)	$K_{Ic}^{(1)}$ (MPam0.5)
15.05	1.18	0.99	0.44	3.76	0.55	1.52	3.17

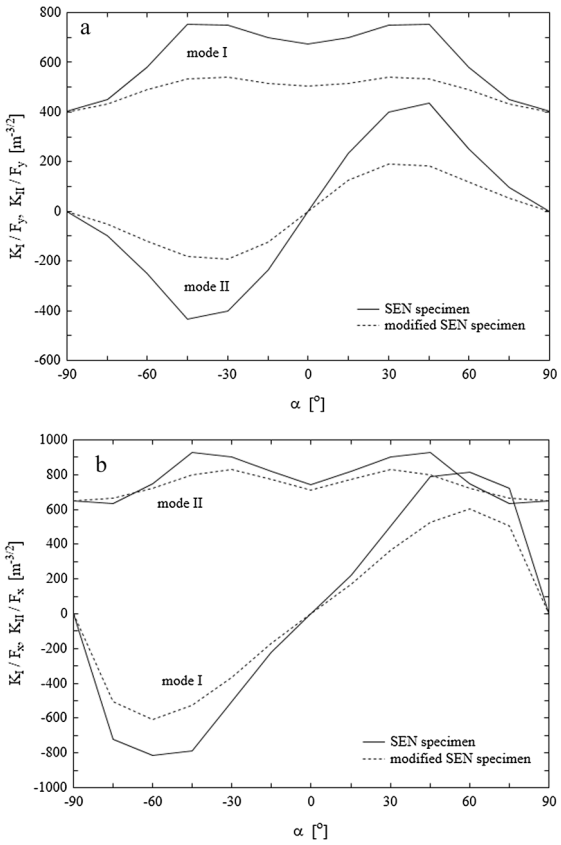

Fig. 2. Variations of the normalized stress intensity factors for: (a) single edge cracked plate under off-axis tensile loading; (b) single edge cracked plate under off-axis shear loading.

4. Results

4.1. Prediction of the direction of crack propagation

The deviation of theoretical values of the crack propagation angle θ_c from experimental values serves as a measure of the correctness of orthotropic fracture criteria. Cracks in highly orthotropic materials such as wood are constrained to propagate along the wood fibers regardless of their original orientation and loading mode mixity because the toughness parallel to fibers $K_{Ic}^{(2)}$ is relative low in comparison to that perpendicular to fibers $K_{Ic}^{(1)}$. This means that there are two possible crack growth directions (α or α - 180°). Experimental evidences indicate that only cracks oriented across the reinforcement direction can split into the two branches.

In order to calculate the direction of crack propagation, the fracture criteria (3) and (6) are normalized by the angular distribution of fracture toughness (13). The critical lengths r_c and d are determined from Eqs. (4) and (7). Variations of the normalized circumferential stress σ_θ^* with and without the T-stress term and the normalized non-local stress function R^* around the crack tip of the specimen are shown in Fig. 4a and 4b for tensile and shear loading, respectively. It can be seen from these figures that locations of the maxima of functions σ_θ^* and R^* representing θ_c vary with material orientation α. It should be noted that the stress curve R^* for $\alpha = 90^\circ$ is symmetrical for both tensile and shear loading, whereas the stress curve σ_θ^* for $\alpha = 90^\circ$ is symmetrical only for tensile loading. Thus, the non-local stress fracture theory predicts that cracks oriented across the reinforcement direction $\alpha = 90^\circ$ propagates either upwards or downwards for both loading modes, whereas the maximum circumferential stress theory with and without T-stress reproduces this behavior only for tensile loading. For other material orientations, the three approaches calculate one value for θ_c.

Fig. 5a and b show a comparison between the crack growth directions computed analytically from the fracture theories and those measured from tests for different material orientations α and two loading modes. In general, theoretical predictions of the direction of

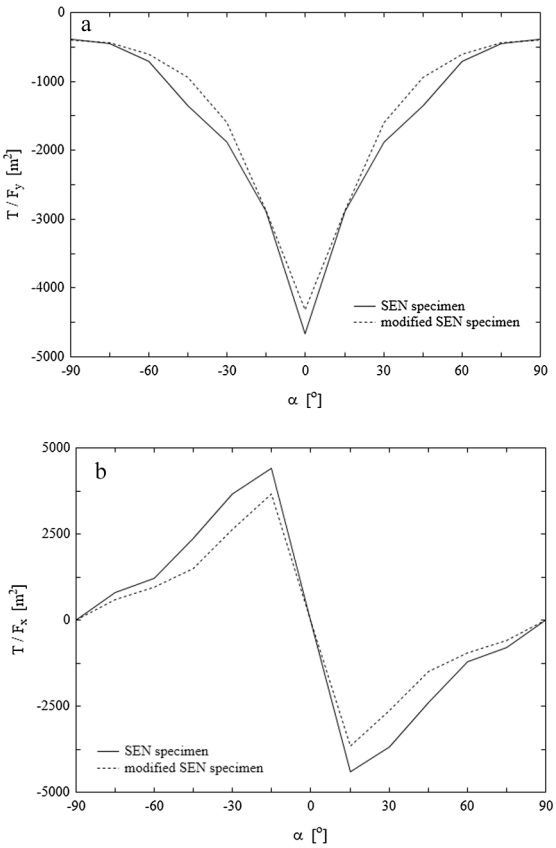

Fig. 3. Variations of the normalized T-stress for: (a) single edge cracked plate under off-axis tensile loading; (b) single edge cracked plate under off-axis shear loading.

crack propagation follow the trend of experimental results. However, the estimation accuracy depends on the material orientation and loading mode. It can be seen from Fig. 5a and b that calculations under tensile loading are in better agreement with measurements for α smaller than 45° whereas predictions under shear loading show better agreement for α larger than 45°. The differences between predictions and experimental data can be explained by the presence of T-stress and shear stress on the critical plane.

Comparing different fracture theories without T-stress, it can be seen that accounting for shear stress in the fracture criterion significantly improves prediction in the case of cracks oriented along the reinforcement direction α = 0° under shear loading. This finding is understandable because fracture mechanism in this case has to be related to shear stress. For other material orientations, the two fracture theories give similar results.

Comparing the same fracture theory with and without T-stress, it can be seen on the one hand, that accounting for T-stress improves prediction of the crack propagation direction in the specimen with material angle α = 22.5° under shear loading, and on the other hand that, it leads to less accurate predictions under tensile loading for α larger than 45°. This is because the computations

Table 2
Values of the biaxial parameter *B*.

Tensile loading (χ = 0°)					
α	0°	22.5°	45°	67.5°	90°
B	−3.09	−0.86	−0.50	−0.30	−0.34
Shear loading (χ = 90°)					
α	0°	22.5°	45°	67.5°	90°
B	0	−1.53	−0.62	−0.34	0

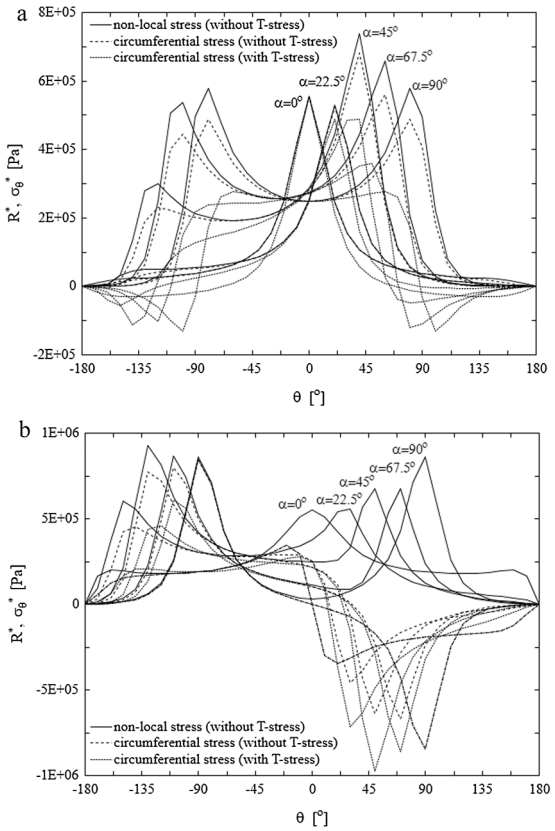

Fig. 4. Variations of the normalized circumferential stress with and without the T-stress term and the normalized non-local stress function around the crack tip for: (a) single edge cracked plate under off-axis tensile loading; (b) single edge cracked plate under off-axis shear loading.

under tensile loading involving T-stress are affected by the critical length r_c. Fig. 6a and 6b show that an increase in the length r_c greatly decreases the crack propagation angle under tensile loading for α larger than 45° and there is no significant effect on the direction of crack propagation under shear loading. This finding suggests that the T-stress effect may play a role in explaining the shear fracture tests in which the crack axis does not coincide with the reinforcement direction.

Summarizing, it can be concluded that the crack propagation direction can be determined with reasonably accuracy by taking into account the anisotropy of fracture toughness and the effects of T-stress and shear stress on material decohesion.

4.2. Prediction of the fracture locus

For mixed mode problems, the fracture locus in the space of stress intensity factors defines the onset of crack growth. For orthotropic materials, the crack stability depends not only on the loading mode mixity, but also on the material orientation. The fracture loci of wood calculated from the two fracture theories are now compared with experimental results obtained from tests on the single edge-notched specimens with different material and loading angles.

The relations between critical values of the stress intensity factors predicted from the maximum circumferential stress theory with and without T-stress are presented in Fig. 7a–c. Theoretical results shown in these figures are computed from linear conditions (5). It can be seen from these figures that the angular distributions of fracture toughness in the form (15) and (16) lead to different fracture predictions for the same fracture problem. Thus, solutions using the mode I fracture toughness along the 1 orthotropy axis $K_{Ic}^{(1)}$ and using that along the 2 orthotropy axis $K_{Ic}^{(2)}$ provide the lower and upper bounds for the fracture loci. The averaged fracture loci obtained from these bounds are shown in Fig. 7a–c. It is interesting to note that the averaged predictions lie closer the experimental data than the lower and upper bounds for each test problem. The inconsistency between the both bounds observed in Fig. 7b for $\alpha = 90^\circ$ may be explained in this way. Under tensile loading, the lower bound crosses the value $K_{Ic}^{(2)}$ for $\alpha = 0^\circ$ because the calculated

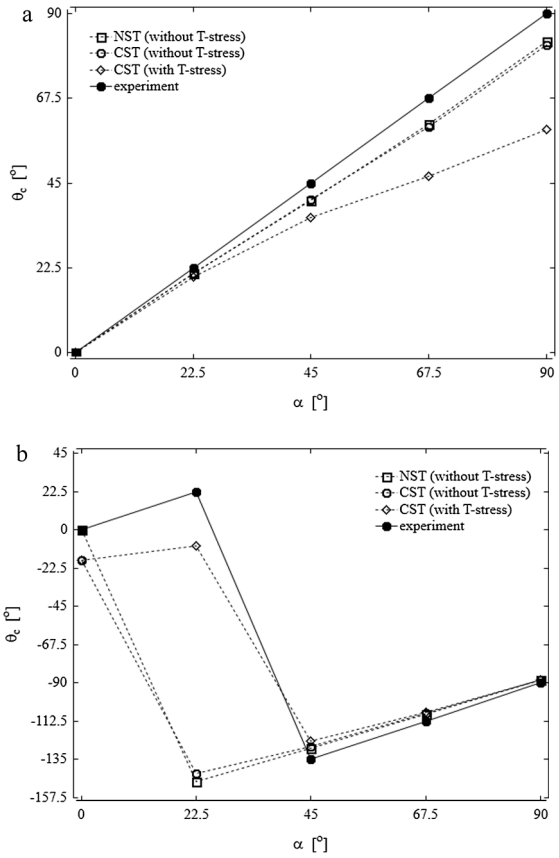

Fig. 5. Comparison of the crack propagation angles obtained from two versions of the maximum circumferential stress criterion with and without T-stress and the non-local stress fracture criterion with experimental data [16] for: (a) single edge cracked plate under off-axis tensile loading; (b) single edge cracked plate under off-axis shear loading.

crack growth angle is the same as that measured in tests $\theta_c = 0^\circ$, whereas the upper bound does not cross the value $K_{Ic}^{(1)}$ for $\alpha = 90^\circ$ because in this case the calculated crack growth angle differs from the measured value $\theta_c = 90^\circ$.

Comparing the fracture loci with and without T-stress, it can be seen that including T-stress overpredicts the measurements for the specimen with material angle $\alpha = 22.5^\circ$ under shear loading and those for $\alpha = 90^\circ$ under tensile loading. For other orientation angles, the criterion with T-stress predicts slightly better than that without T-stress. However, the differences between the fracture loci with and without T-stress are less than the differences between the lower and upper bounds. This finding suggests that the anisotropy of fracture toughness has a stronger effect on material decohesion than T-stress, except for the two cases mentioned above. As expected, including T-stress has no influence on the fracture locus in the case of cracks oriented along the reinforcement direction (Fig. 7a). This is because for $\alpha = 0^\circ$, either the value of T-stress is zero (under pure sliding fracture mode) or the value of θ_c is zero (under pure opening fracture mode). In this case, $\theta_c = 0^\circ$ means that a term $T\sin^2\theta$ occurring in the fracture criterion disappears.

The relations between critical values of the stress intensity factors obtained from the non-local stress fracture theory for different material configurations and loading modes are presented in Fig. 8a–c together with the averaged loci from the maximum circumferential stress theory without T-stress. The non-local stress predictions are computed from elliptical conditions (10). Graphically, the solutions lie on rotated ellipses below the major axes for tensile loading whereas for shear loading, they are placed above the major axes. Rotations of ellipses (10) were discussed in detail in Ref. [16] and will not be repeated here. For normalization purpose, the angular distribution of fracture toughness related to $K_{Ic}^{(2)}$ is only used in the non-local stress fracture theory. This is because the solutions for critical stress intensity factors obtained by using $K_{Ic}^{(1)}$ are complex numbers. Comparing the fracture loci obtained from the two theories with experimental data, it can be seen that the non-local stress fracture criterion correlates better with measurements than the averaged circumferential stress criterion for each test problem. Fig. 8a–c show that the nonlocal stress predictions give the exact values of $K_{Ic}^{(2)}$ and $K_{IIc}^{(2)}$, whereas the maximum circumferential stress predictions averaged from the two bounds do not.

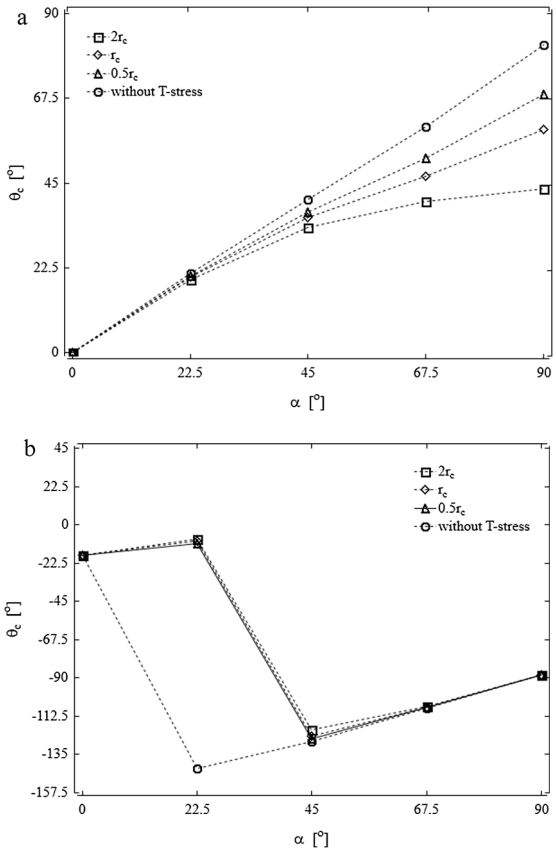

Fig. 6. Influence of different critical lengths r_c on the crack propagation angle predicted from the maximum circumferential stress criterion for: (a) single edge cracked plate under off-axis tensile loading; (b) single edge cracked plate under off-axis shear loading.

Comparing among different test problems, it can be observed that the non-local stress predictions for specimens with cracks inclined to the reinforcement direction under shear loading (Fig. 8c) are less accurate than those under tensile loading (Fig. 8b) and those for specimens with cracks oriented along the reinforcement direction (Fig. 8a). This finding can be attributed to the fact that the shear fracture tests in which the crack axis does not coincide with the reinforcement direction are more affected by T-stress than other types of fracture tests (see Table 2).

Fig. 8a–c show also a comparison between the fracture loci obtained from the non-local stress fracture theory using strict and simplified approaches for determining the crack propagation angle θ_c. The first presented above takes the angular variation of the fracture toughness into account (15) and the second reported in Ref. [16] assumes that the crack propagation angles are known a priori (11). As expected, the latter approach calculates the onset of crack growth closer to experimental data obtained from tests in which the crack axis does not coincide with the reinforcement direction for both tensile and shear loading. It is interesting to note that both approaches give the same results in the case of fracture tests in which the crack axis and the reinforcement direction coincide (Fig. 8a) because they predict in this case the same values of the crack propagation angle. The differences between the strict and simplified fracture loci can be regarded as errors in the approximation of the angular distributions of fracture toughness. Because the strict approach is based on the angular distribution related to $K_{Ic}^{(2)}$, it is understandable that the maximum error of approximation occurs under tensile loading for $\alpha = 90^\circ$.

5. Conclusions

A comparative study between the maximum circumferential stress and non-local stress theories is presented in this paper to assess the range of validity of the two fracture criteria for predicting the crack propagation direction and critical load in orthotropic materials. The predictions from the two fracture theories are compared with experimental results available in the literature on mixed mode fracture of wood.

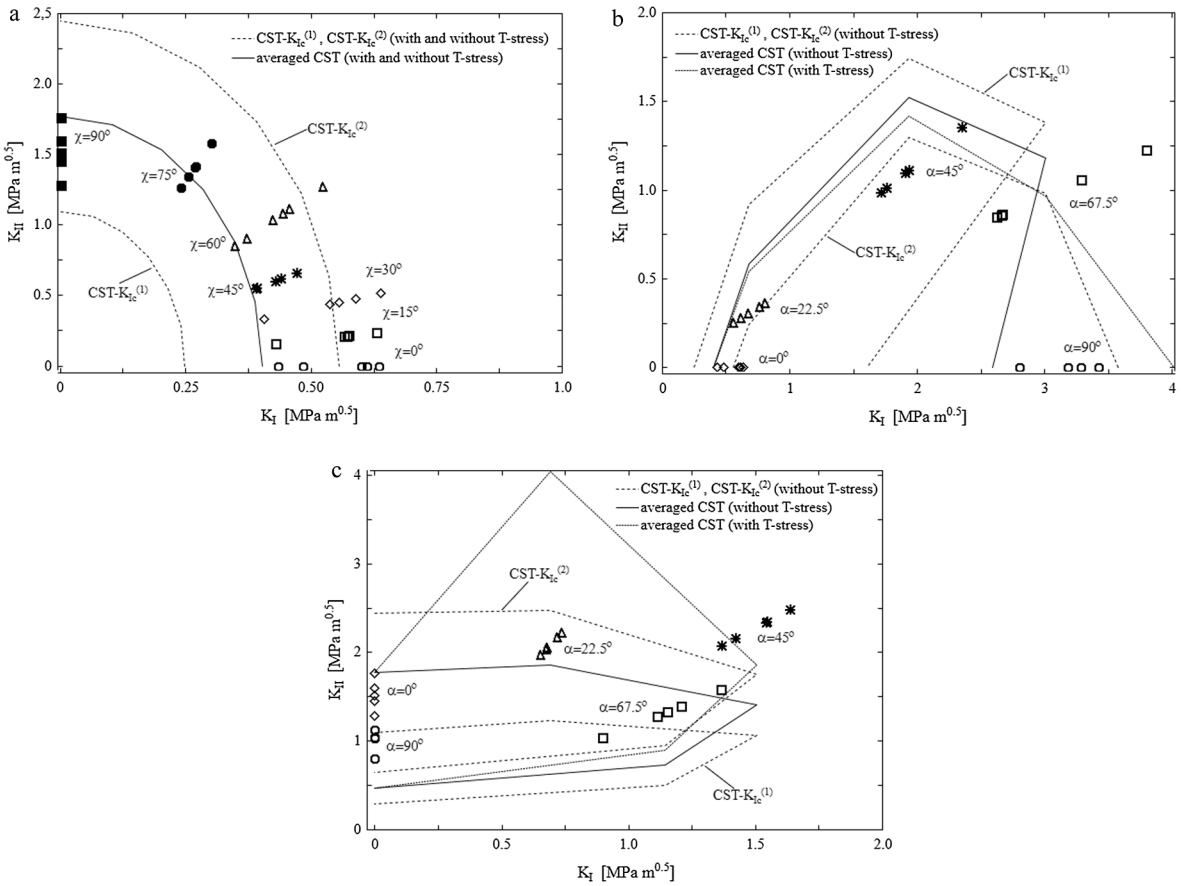

Fig. 7. Comparison of the fracture loci obtained from different versions of the maximum circumferential stress criterion with experimental data [16] for: (a) single edge cracked plate under on-axis biaxial loading; (b) single edge cracked plate under off-axis tensile loading; (c) single edge cracked plate under off-axis shear loading.

A version of the maximum circumferential stress criterion based on the simplified angular distribution of fracture toughness related only to the mode I fracture toughness for a crack located along the reinforcement direction, which is commonly found in the literature, underpredicts the fracture loci of wood. The prediction accuracy improves when both mode I fracture toughnesses for cracks located along and across the reinforcement direction are incorporated into this fracture model. It was demonstrated that the mode I fracture toughnesses used separately provide the lower and upper bounds for the fracture loci.

The main drawback of the maximum circumferential stress theory is that it predicts non-collinear crack growth under pure sliding fracture mode in the case of cracks oriented along the reinforcement direction. As a result of this, this fracture theory fails to predict correctly the fracture loci of wood. However, due to the simplicity of this approach, it can be easily extended to include the T-stress effect. The results of this investigation show that including T-stress into the maximum circumferential stress criterion improves predictions of the crack propagation direction under shear loading when high values of T-stress occur but it is not sufficient to guarantee the consistency of the predicted critical loads with measurements.

Although the non-local stress fracture criterion is not suitable for modeling the T-stress effect, it reproduces collinear crack growth for cracks oriented along the reinforcement direction under both tensile and shear loading. It was demonstrated that the fracture loci obtained from the elliptical criterion for different mixed mode problems agree better with measurements than that predicted from the maximum circumferential stress theory. Taking the above into account, it can be concluded that the fracture process in wood is influenced by shear stress acting on the critical plane and that the shear stress component should not be neglected in the fracture model. The results of this study show that the simplified theory based on a concept of weak planes parallel to the reinforcement direction can be an alternative to the strict non-local stress theory including the anisotropy of fracture toughness, however it is not capable of explaining the entire fracture behavior.

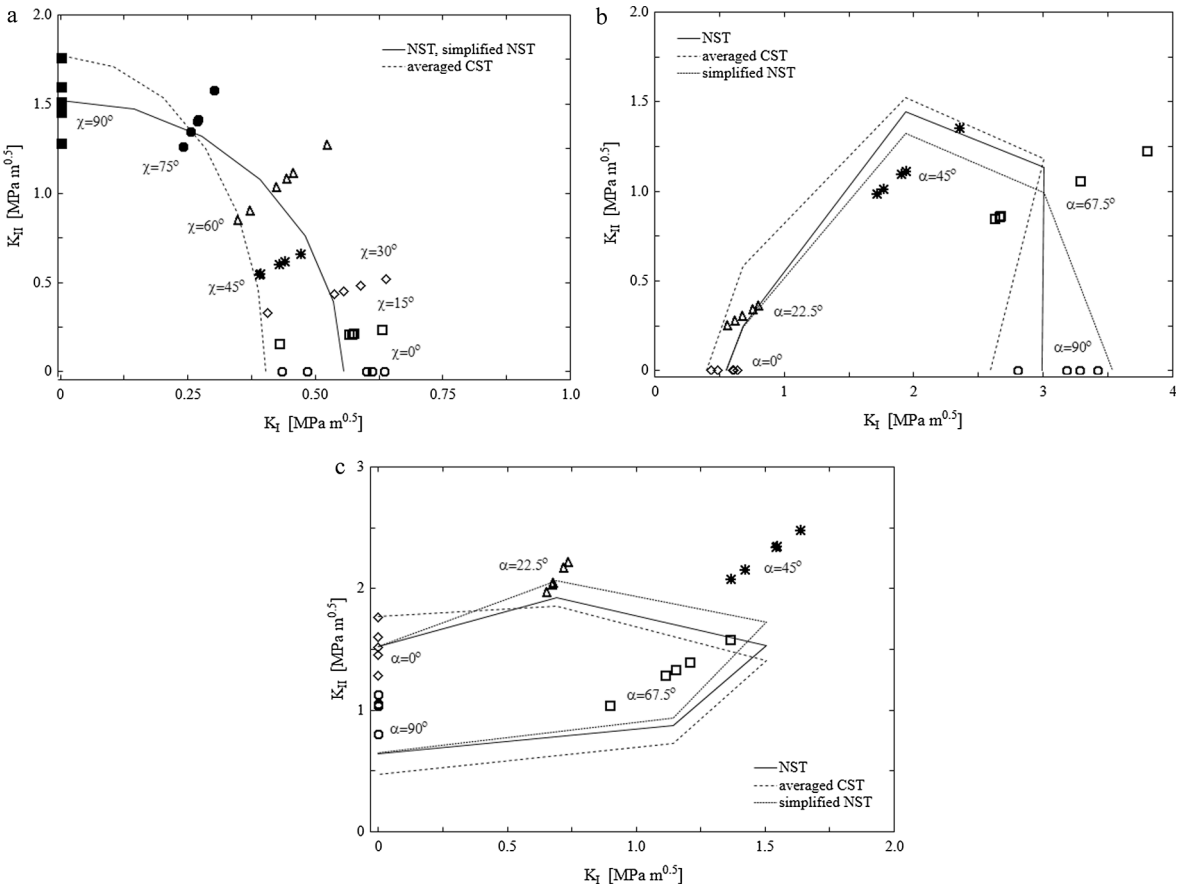

Fig. 8. Comparison of the fracture loci obtained from the strict and simplified versions of the non-local stress fracture criterion and the maximum circumferential stress criterion averaged from the lower and upper bounds with experimental data [16] for: (a) single edge cracked plate under on-axis biaxial loading; (b) single edge cracked plate under off-axis tensile loading; (c) single edge cracked plate under off-axis shear loading.

Acknowledgement

The research described here was financially supported by the Ministry of Science and Higher Education of Poland under the grant No. S/WM/4/2017.

Appendix A. Asymptotic stress fields in the vicinity of the crack tip in a orthotropic material

Sih et al. [25] obtained the following expressions for the stress fields in the vicinity of the crack tip in a orthotropic material

$$\sigma_x = \frac{K_I}{\sqrt{2\pi r}} F_{Ix}(\theta, \mu_1, \mu_2) + \frac{K_{II}}{\sqrt{2\pi r}} F_{IIx}(\theta, \mu_1, \mu_2) + T \tag{A1}$$

$$\sigma_y = \frac{K_I}{\sqrt{2\pi r}} F_{Iy}(\theta, \mu_1, \mu_2) + \frac{K_{II}}{\sqrt{2\pi r}} F_{IIy}(\theta, \mu_1, \mu_2) \tag{A2}$$

$$\tau_{xy} = \frac{K_I}{\sqrt{2\pi r}} F_{Ixy}(\theta, \mu_1, \mu_2) + \frac{K_{II}}{\sqrt{2\pi r}} F_{IIxy}(\theta, \mu_1, \mu_2) \tag{A3}$$

where r, θ are polar coordinates originating from the crack tip in the xy plane, K_I, K_{II} are the stress intensity factors, T is the non-singular term (T-stress) which acts parallel to a crack. Functions $F_{Ix}(\theta, \mu_1, \mu_2) \cdots F_{IIxy}(\theta, \mu_1, \mu_2)$ are given by**

$$F_{Ix}(\theta, \mu_1, \mu_2) = \mathrm{Re}\left[\frac{\mu_1\mu_2}{\mu_1 - \mu_2}\left(\frac{\mu_2}{\sqrt{\cos\theta + \mu_2 \sin\theta}} - \frac{\mu_1}{\sqrt{\cos\theta + \mu_1 \sin\theta}}\right)\right] \tag{A4}$$

$$F_{Iy}(\theta, \mu_1, \mu_2) = \mathrm{Re}\left[\frac{1}{\mu_1 - \mu_2}\left(\frac{\mu_1}{\sqrt{\cos\theta + \mu_2 \sin\theta}} - \frac{\mu_2}{\sqrt{\cos\theta + \mu_1 \sin\theta}}\right)\right] \tag{A5}$$

$$F_{\mathrm{I}xy}(\theta,\mu_1,\mu_2)=\mathrm{Re}\left[\frac{\mu_1\mu_2}{\mu_1-\mu_2}\left(\frac{1}{\sqrt{\cos\theta+\mu_1\sin\theta}}-\frac{1}{\sqrt{\cos\theta+\mu_2\sin\theta}}\right)\right] \tag{A6}$$

$$F_{\mathrm{II}x}(\theta,\mu_1,\mu_2)=\mathrm{Re}\left[\frac{1}{\mu_1-\mu_2}\left(\frac{(\mu_2)^2}{\sqrt{\cos\theta+\mu_2\sin\theta}}-\frac{(\mu_1)^2}{\sqrt{\cos\theta+\mu_1\sin\theta}}\right)\right] \tag{A7}$$

$$F_{\mathrm{II}y}(\theta,\mu_1,\mu_2)=\mathrm{Re}\left[\frac{1}{\mu_1-\mu_2}\left(\frac{1}{\sqrt{\cos\theta+\mu_2\sin\theta}}-\frac{1}{\sqrt{\cos\theta+\mu_1\sin\theta}}\right)\right] \tag{A8}$$

$$F_{\mathrm{II}xy}(\theta,\mu_1,\mu_2)=\mathrm{Re}\left[\frac{1}{\mu_1-\mu_2}\left(\frac{\mu_1}{\sqrt{\cos\theta+\mu_1\sin\theta}}-\frac{\mu_2}{\sqrt{\cos\theta+\mu_2\sin\theta}}\right)\right] \tag{A9}$$

where μ_1, μ_2 are roots of the characteristic equation [26]

$$a_{11}\mu^4-2a_{16}\mu^3+(2a_{12}+a_{66})\mu^2-2a_{26}\mu+a_{22}=0 \tag{A10}$$

with positive imaginary part and $a_{11}\ldots a_{22}$ are elements of the compliance matrix which relate stress to strain in the xy coordinate system according to the generalized Hooke's law

$$\begin{Bmatrix}\varepsilon_x\\ \varepsilon_y\\ \gamma_{xy}\end{Bmatrix}=\begin{bmatrix}a_{11} & a_{12} & a_{16}\\ a_{12} & a_{22} & a_{26}\\ a_{16} & a_{26} & a_{66}\end{bmatrix}\begin{Bmatrix}\sigma_x\\ \sigma_y\\ \tau_{xy}\end{Bmatrix} \tag{A11}$$

Appendix B. Displacement extrapolation method

Saouma and Sikiotis [27] and Boone et al. [28] presented displacement extrapolation method for calculating the stress intensity factors in a orthotropic material in which they assumed correlation between the displacements in singular quarter point elements and the theoretical values. Recently, this technique was also used to evaluate T-stress in a orthotropic material by Sladek et al. [29] and Tran and Mear [30]. Following Sih et al. [25], analytical displacement fields in the vicinity of the crack tip are given by

$$u=\sqrt{\frac{2r}{\pi}}K_{\mathrm{I}}F_{\mathrm{I}u}(\theta,\mu_1,\mu_2)+\sqrt{\frac{2r}{\pi}}K_{\mathrm{II}}F_{\mathrm{II}u}(\theta,\mu_1,\mu_2)+a_{11}Tr\cos\theta \tag{B1}$$

$$v=\sqrt{\frac{2r}{\pi}}K_{\mathrm{I}}F_{\mathrm{I}v}(\theta,\mu_1,\mu_2)+\sqrt{\frac{2r}{\pi}}K_{\mathrm{II}}F_{\mathrm{II}v}(\theta,\mu_1,\mu_2)+a_{12}Tr\sin\theta \tag{B2}$$

Functions $F_{\mathrm{I}u}(\theta,\mu_1,\mu_2)\cdots F_{\mathrm{II}v}(\theta,\mu_1,\mu_2)$ are defined as follows

$$F_{\mathrm{I}u}(\theta,\mu_1,\mu_2)=\mathrm{Re}\left[\frac{1}{\mu_1-\mu_2}(\mu_1p_2\sqrt{\cos\theta+\mu_2\sin\theta}-\mu_2p_1\sqrt{\cos\theta+\mu_1\sin\theta})\right] \tag{B3}$$

$$F_{\mathrm{II}u}(\theta,\mu_1,\mu_2)=\mathrm{Re}\left[\frac{1}{\mu_1-\mu_2}(p_2\sqrt{\cos\theta+\mu_2\sin\theta}-p_1\sqrt{\cos\theta+\mu_1\sin\theta})\right] \tag{B4}$$

$$F_{\mathrm{I}v}(\theta,\mu_1,\mu_2)=\mathrm{Re}\left[\frac{1}{\mu_1-\mu_2}(\mu_1q_2\sqrt{\cos\theta+\mu_2\sin\theta}-\mu_2q_1\sqrt{\cos\theta+\mu_1\sin\theta})\right] \tag{B5}$$

$$F_{\mathrm{II}v}(\theta,\mu_1,\mu_2)=\mathrm{Re}\left[\frac{1}{\mu_1-\mu_2}(q_2\sqrt{\cos\theta+\mu_2\sin\theta}-q_1\sqrt{\cos\theta+\mu_1\sin\theta})\right] \tag{B6}$$

where

$$p_1=a_{11}(\mu_1)^2+a_{12}-a_{16}\mu_1,\qquad p_2=a_{11}(\mu_2)^2+a_{12}-a_{16}\mu_2 \tag{B7}$$

$$q_1=a_{12}\mu_1+\frac{a_{22}}{\mu_1}-a_{26},\qquad q_2=a_{12}\mu_2+\frac{a_{22}}{\mu_2}-a_{26} \tag{B8}$$

Using equations (B1)–(B8), the relative difference of the crack face displacements is derived in the matrix notation as follows

$$\begin{Bmatrix}u(\theta=+\pi)-u(\theta=-\pi)\\ v(\theta=+\pi)-v(\theta=-\pi)\end{Bmatrix}=2\sqrt{\frac{2r}{\pi}}\begin{bmatrix}F_{\mathrm{I}u}(\theta=\pm\pi) & F_{\mathrm{II}u}(\theta=\pm\pi)\\ F_{\mathrm{I}v}(\theta=\pm\pi) & F_{\mathrm{II}v}(\theta=\pm\pi)\end{bmatrix}\begin{Bmatrix}K_{\mathrm{I}}\\ K_{\mathrm{II}}\end{Bmatrix} \tag{B9}$$

and the sum of the crack-face displacements is expressed as

$$\begin{Bmatrix} u(\theta=+\pi)+u(\theta=-\pi) \\ v(\theta=+\pi)+v(\theta=-\pi) \end{Bmatrix} = \begin{Bmatrix} -2a_{11}Tr \\ 0 \end{Bmatrix} \tag{B10}$$

Using singular quarter point elements, the crack face displacements are approximated by

$$u(\theta=+\pi) = u_1 + (-3u_1 + 4u_2 - u_3)\sqrt{\frac{r}{L}} + 2(u_1 - 2u_2 + u_3)\frac{r}{L} \tag{B11}$$

$$u(\theta=-\pi) = u_1 + (-3u_1 + 4u_4 - u_5)\sqrt{\frac{r}{L}} + 2(u_1 - 2u_4 + u_5)\frac{r}{L} \tag{B12}$$

$$v(\theta=+\pi) = v_1 + (-3v_1 + 4v_2 - v_3)\sqrt{\frac{r}{L}} + 2(v_1 - 2v_2 + v_3)\frac{r}{L} \tag{B13}$$

$$v(\theta=-\pi) = v_1 + (-3v_1 + 4v_4 - v_5)\sqrt{\frac{r}{L}} + 2(v_1 - 2v_4 + v_5)\frac{r}{L} \tag{B14}$$

where u_1, v_1 are values of the node displacements at the crack tip in the x and y directions, respectively, u_2, v_2 and u_4, v_4 are values of the quarter node displacements, u_3, v_3 and u_5, v_5 are values of the node displacements at the distance L from the crack tip. Substituting equations (B11)–(B14) into Eqs. (B9) and (B10) and equating the terms with identical powers of r leads to the following expressions for the stress intensity factors

$$\begin{Bmatrix} K_I \\ K_{II} \end{Bmatrix} = \frac{1}{2}\sqrt{\frac{\pi}{2L}} \begin{bmatrix} F_{Iu}(\theta=\pm\pi) & F_{IIu}(\theta=\pm\pi) \\ F_{Iv}(\theta=\pm\pi) & F_{IIv}(\theta=\pm\pi) \end{bmatrix}^{-1} \begin{Bmatrix} 4(u_6-u_4)-(u_3-u_5) \\ 4(v_6-v_4)-(v_3-v_5) \end{Bmatrix} \tag{B15}$$

and T-stress

$$T = -\left[\frac{2(u_1 - 2u_2 + u_3) + 2(u_1 - 2u_4 + u_5)}{2a_{11}L}\right] \tag{B16}$$

In order to verify the accuracy of the method, the problem an inclined center crack of length $2a$ located in an infinite orthotropic plate subjected to far-field constant traction σ was considered. For this crack problem, there are analytical solutions for stress intensity factors [25] and T-stress [31]. The material properties and plate geometries employed here are the same as those used by Kim and Paulino [32] for calculating T-stress by means of the interaction integral. Table 3 shows that the estimates obtained for $a/L = 30$ from the displacement extrapolation method are in good agreement with the benchmark solutions.

Table 3
Values of the stress intensity factors and T-stress for the orthotropic plate containing a central angled crack.

	Present	Present	Exact solution [25]	Exact solution [25]	Present	Exact solution [31]	Interaction integral [32]
Crack inclination	$K_I/\sigma\sqrt{\pi a}$	$K_{II}/\sigma\sqrt{\pi a}$	$K_I/\sigma\sqrt{\pi a}$	$K_{II}/\sigma\sqrt{\pi a}$	T/σ	T/σ	T/σ
0°	1.011	0	1	0	−2.985	−3.162	−3.164
15°	0.947	0.241	0.933	0.250	−1.588	x	−1.643
30°	0.767	0.424	0.750	0.433	0.076	x	0.031
45°	0.511	0.504	0.500	0.500	0.709	x	0.716
60°	0.260	0.440	0.250	0.433	0.941	x	0.936
75°	0.069	0.255	0.067	0.250	0.991	x	0.988
90°	0	0	0	0	1	1	0.996

References

[1] van der Put TACM. A new fracture mechanics theory for orthotropic materials like wood. Eng Fract Mech 2007;74:771–81.
[2] Fakoor M, Shokrollahim MS. A new macro-mechanical approach for investigation of damage zone effects on mixed mode I/II fracture of orthotropic materials. Acta Mech 2018;229:3537–56.
[3] Fakoor M, Khansari NM. General mixed mode I/II failure criterion for composite materials based on matrix fracture properties. Theor Appl Fract Mech 2018;96:428–42.
[4] Fakoor M. Augmented Strain Energy Release Rate (ASER): a novel approach for investigation of mixed-mode I/II fracture of composite materials. Eng Fract Mech 2017;179:177–89.
[5] Erdogan F, Sih GC. On the crack extension in plates under plane loading and transverse shear. J Basic Eng 1963:519–27.
[6] Seweryn A, Mroz Z. A non-local stress failure condition for structural elements under multiaxial loading. Eng Fract Mech 1995;51:955–73.
[7] Buczek MB, Herakovich CT. A normal stress criterion for crack extension direction in orthotropic materials. J Compost Mater 1985;19:544–53.
[8] Saouma V, Ayari ML, Leavell D. Mixed mode crack propagation in homogeneous anisotropic solids. Eng Fract Mech 1987;27:171–84.
[9] Cahill LMA, Natarajan S, Bordas SPA, O'Higgins RM, McCarthy CT. An experimental/numerical investigation into the main driving force for crack propagation in uni-directional fibre-reinforced composite laminae. Compos Struct 2014;107:119–30.
[10] Bayesteh H, Mohammadi S. XFEM fracture analysis of orthotropic functionally graded materials. Compos: Part B 2013;44:8–25.
[11] Arakere NK, Knudsen EC, Wells D, McGill P, Swanson GR. Determination of mixed-mode stress intensity factors, fracture toughness, and crack turning angle for anisotropic foam material. Inter J Solids Struct 2008;45:4936–51.

[12] Nobile L, Carloni C. Fracture analysis for orthotropic cracked plates. Compos Struct 2005;68:285–93.
[13] Lim WK, Choi SY, Sankar BV. Biaxial load effects on crack extension in anisotropic solids. Eng Fract Mech 2001;68:403–16.
[14] Lim WK. Mixed-mode crack extension in orthotropic materials under biaxial load. Int J Fract 2012;173:71–7.
[15] Jernkvist LO. Fracture of wood under mixed mode loading, I Derivation of fracture criteria. Eng Fract Mech 2001;68:549–63.
[16] Romanowicz M, Seweryn A. Verification of a non-local stress criterion for mixed mode fracture in wood. Eng Fract Mech 2008;75:3141–60.
[17] Anaraki ARG, Fakoor M. General mixed mode I/II fracture criterion for wood considering T-stress effects. Mater Des 2010;31:4461–9.
[18] Anaraki ARG, Fakoor M. Mixed mode fracture criterion for wood based on a reinforcement microcrack damage model. Mater Sci Eng A 2010;527:7184–91.
[19] Wu EM. Application of fracture mechanics to anisotropic plates. J Appl Mech 1967;34:967–74.
[20] de Moura MFSF, Oliveira JMQ, Morais JJL, Xavier J. Mixed-mode I/II wood fracture characterization using the mixed-mode bending test. Eng Fract Mech 2010;77:144–52.
[21] Phan NA, Morel S, Chaplain M. Mixed-mode fracture in a quasi-brittle material: R-curve and fracture criterion – application to wood. Eng Fract Mech 2016;156:96–113.
[22] Seweryn A, Kulchytsky-Zhyhailo RD, Mroz Z. On the modeling of bodies with microcracks taking into account of contact of their boundaries. Appl Probl Mech Math 2003;1:141–9.
[23] Mroz Z, Seweryn A. Non-local failure and damage evolution rule : application to a dilatant crack model. J Phys IV 1998;8:257–68.
[24] Leevers PS, Radon JC. Inherent stress biaxiality in various fracture specimen geometries. Int J. Fract 1982;19:311–25.
[25] Sih GC, Paris PC, Irwin GR. On cracks in rectilinearly anisotropic bodies. Int J Fract 1965;3:189–203.
[26] Lekhnicki SG. Theory of elasticity of an anisotropic elastic body. San Francisco: Holden-Day Inc.; 1963.
[27] Saouma VE, Sikiotis EF. Stress intensity factors in anisotropic bodies using singular isoparametric elements. Eng Fract Mech 1986;25:115–21.
[28] Boone TJ, Wawrzynek PA, Ingraffea AR. Finite element modeling of fracture propagation in orthotropic materials. Eng Fract Mech 1987;26:185–201.
[29] Sladek J, Sladek V, Repka M, Tan CL. Evaluation of the T-stress for cracks in functionally graded materials by the FEM. Theor Appl Fract Mech 2016;86:332–41.
[30] Tran HD, Mear ME. Calculation of T-stress for cracks in two-dimensional anisotropic elastic media by boundary integral equation method. Int J Fract 2018;211:149–62.
[31] Gao H, Chiu CH. Slightly curved or kinked cracks in anisotropic elastic solids. Int J Solids Struct 1992;29:947–72.
[32] Kim JH, Paulino GH. T-stress in orthotropic functionally graded materials: Lekhnitskii and Stroh formalisms. Int J Fract 2004;126:345–84.